Polymer Chemistry

Diblock brush-arm star copolymers via a core-first/graft-from approach using γ-cyclodextrin and ROMP: a modular platform for drug delivery

Journal:	*Polymer Chemistry*
Manuscript ID	PY-ART-08-2019-001146.R1
Article Type:	Paper
Date Submitted by the Author:	06-Oct-2019
Complete List of Authors:	Li, Ruihan; Washington University in Saint Louis, ; Li, Xuesong; Washington University in St. Louis, Chemistry Zhang, Yipei; Washington University in St. Louis, Chemistry Delawder, Abigail; Washington University in St. Louis, Chemistry Colley, Nathan; Washington University in Saint Louis, ; Southern Illinois University Carbondale, Whiting, Emma; Washington University in St. Louis, Chemistry Barnes, Jonathan; Washington University in St. Louis, Chemistry

ARTICLE

Diblock brush-arm star copolymers via a core-first/graft-from approach using γ-cyclodextrin and ROMP: a modular platform for drug delivery

Received 31st July 2019,
Accepted 00th XXXX 20xx

DOI: 10.1039/x0xx00000x

Ruihan Li,[†,a] Xuesong Li,[†,a] Yipei Zhang,[a] Abigail O. Delawder,[a] Nathan D. Colley,[a] Emma A. Whiting,[a] Jonathan C. Barnes*[a]

The design and synthesis of a novel multifunctional core initiator based on γ-cyclodextrin (γ-CD) functionalized with eight norbornenes is reported, and a core-first approach to make eight-arm star polymers using ring-opening metathesis polymerization is carried out by grafting-from the initiator using norbornene-functionalized hexaethylene glycol. The living nature of the polymerization was verified through chain extension of the ω-functional arms with norbornene-functionalized poly(ethylene glycol) (PEG, M_n ≈ 2 kDa) to generate water-soluble diblock brush-arm star copolymers (DBASCs) with high molar masses ($M_{n,NMR}$ = 187–268 kDa) and low dispersities ($Đ$ = 1.12–1.19). The size of the corresponding star polymers was confirmed by transmission electron microscopy and dynamic light scattering (D_h ≈ 10.0–11.0 nm). The thermal properties (e.g., T_g) of the DBASCs were determined by thermal gravimetric analysis and differential scanning calorimetry, the latter of which showed well-ordered materials in the solid state (prominent T_c and T_m peaks). The long-range order and crystallinity of solid-state DBASCs was further supported by well-defined powder X-ray diffraction patterns. Lastly, since γ-CD possesses an order of magnitude greater solubility in water and enhanced drug-binding capabilities compared to that for β-CD, a representative DBASC was evaluated against healthy human umbilical vein endothelial cells (and exhibited low toxicity), and was also investigated as a delivery vehicle for the anticancer drug doxorubicin as its hydrochloride salt (DOX·HCl), resulting in greater potency against MCF-7 breast cancer cells relative to that of the free DOX·HCl treatment. The star polymers reported herein represent a new modular polymeric platform with potential applications in nanostructure self-assembly and drug delivery.

Introduction

Star polymers[1, 2] consist of a central core connecting three or more linear polymers that radiate outwards from a central point. This branched, arm-like architecture imbues star polymers with solution and bulk properties[3] that are distinct from their linear analogues, and thus sets the stage for a variety of unique nanomaterial applications,[4] such as self-assembly,[5] drug delivery,[6, 7] catalysis,[8, 9] and so on. The two main synthetic approaches to prepare star polymers employ "arm-first" or "core-first" strategies, where the linear polymer arms are generated and then crosslinked by a multifunctional crosslinker, or the arms are grown off an existing multifunctional core initiator, respectively. Many different types of complex star polymers have been synthesized using these approaches, where arms with block,[10-12] mikto,[13, 14] and bottlebrush[15, 16] architectures have been prepared using a wide range of living polymerization methods that include ionic,[3, 17-21] ring-opening,[22, 23] and controlled radical[24-29] polym-erizations.

In the core-first approach, many multifunctional initiators have been adopted, such as polyols, dendrimers, metal complexes, or cores terminated with multiple bromides or chain-transfer agents.[2] Macrocycles have also been used as multifunctional core initiators, where crown ethers,[30, 31] cucurbit[*n*]uril,[32] calix[*n*]arene,[33] and α-[12, 34] and β-[35] cyclodextrins (CDs) have been employed. These macrocyclic core initiators offer a prearranged display of functional groups that can be easily functionalized and used for growing the corresponding arms of the star polymer. Owing to their biocompatibility, biodegradability, and low toxicities in humans and animals, CDs have been investigated extensively in pharmaceutical applications,[36] and as such, have been used as the multifunctional core initiator in star polymers more than any other class of macrocycles. They also possess the advantage of having an empty hydrophobic cavity at the centre of the macrocycle – with diameters of 4.7–5.3 and 6.0–6.5 Å for α- and β-CD, respectively[37] – which is useful for binding hydrophobic drugs or imaging agents.

Atom transfer radical polymerization (ATRP),[38-41] is the most frequently used polymerization method to synthesize the arms of star polymers possessing macrocyclic cores, where the alcohol or phenolic groups of the macrocycles are usually functionalized with a halide-terminated initiator and the degree of branching in the star polymer depends on the number of installed initiator groups. For example, Matyjaszewski and co-workers recently demonstrated the successful polymerization of a β-CD-based star polymer by carrying out simplified electrochemical ATRP (*se*ATRP) to produce both 14-

[a] *Department of Chemistry, One Brookings Drive, Washington University, St. Louis, MO 63130, USA. E-mail: jcbarnes@wustl.edu*
[†]These authors contributed equally.
Electronic Supplementary Information (ESI) available: Full synthetic protocols, purification and characterization data for all compounds and polymers, and cytotoxicity and anticancer efficacy of star polymers. See DOI: 10.1039/x0xx00000x

and 21-arm star polymers.[42] Likewise, a large number of β-CD-based star polymers have been synthesized previously using ATRP,[6, 12, 35, 43-54] in addition to others prepared using reversible addition-fragmentation chain-transfer (RAFT) polymerization,[55, 56] ring-opening polymerization,[57-61] and the grafting-to method.[34, 62] The larger γ-CD macrocycle, which possesses eight *D*-glucopyranoside rings, an inner cavity of 7.5–8.3 Å, and is an order of magnitude more soluble in water than β-CD, has only been used sparingly by two research groups thus far to synthesize star polymers.[45-47, 63, 64]

Ring-opening metathesis polymerization (ROMP)[65-69] is an efficient, functional group-tolerant method of polymerization that has been used previously to produce diverse polymer architectures.[70-75] To the best of our knowledge, ROMP has never been used to synthesize macrocycle-based star polymers.[54] Instead, ROMP has primarily been used in arm-first[76-78] and brush-first[79-87] strategies to generate star polymers – where the linear or bottlebrush polymer was crosslinked with a bis-norbornene crosslinker – or in a hybrid arm-first/core-first strategy[88] that was used to prepare end-functionalized star polymers.[88-92] In principle, a core-first strategy should provide greater control over the number of protruding arms and reduce potential star-star coupling.

Herein, we report a novel core-first/graft-from ROMP-based synthesis of a diblock brush-arm star copolymer (DBASC) comprising a γ-CD core and eight diblock polynorbornene arms bearing side chains of hexaethylene glycol (HEG) and poly(ethylene glycol) (PEG, $M_n \approx 2$ kDa). The synthesis of the multifunctional initiator – namely, γ-CD functionalized with eight norbornene groups (**γ-CD-Nb$_8$**) – is described, as well as the efficiency of polymerization for each arm as higher monomer-initiator ratios were investigated. The living nature of the star polymer synthesis was also demonstrated by chain extension of the ω-functional arms with a PEG-based macromonomer (**Nb-PEG**), resulting in high molar mass star polymers with low dispersities. Additionally, the size, thermal properties, crystallinity, cytotoxicity, and ability of the γ-CD-based star polymer to function as a drug delivery vehicle is described.

Experimental

Procedure for synthesis of γ-cyclodextrin initiator

γ-CD-I$_8$. Using a previous protocol,[93] a modified method was employed here to synthesize the iodinated initiator precursor. A solution of I_2 (3.60 g, 14.17 mmol, 15.32 equiv.) in DMF (anhydrous, 4.6 mL) was slowly added to a solution of PPh_3 (3.62 g, 13.80 mmol, 14.92 equiv.) in DMF (anhydrous,18 mL) at ambient temperature. After stirring for 30 min, γ-CD (1.2 g, 0.925 mmol, 1 equiv.) was added. The reaction was heated up to 70 °C and stirred for 24 h. After cooling down, a suspension of CH_3ONa (0.87 g, 16.10 mmol, 17.41 equiv.) in CH_3OH (6 mL) was added dropwise and stirred at ambient temperature for 30 min to quench the reaction. Once completed, the organic solvent was removed. The crude material was re-dissolved in a minimal amount of DMF and precipitated by adding Me_2CO. The precipitation was performed three times to yield the desired compound as a white powder. (1.2 g, 59% yield). ^{1}H NMR (500 MHz, $(CD_3)_2SO$): δ_H 5.97 (s, 16H), 5.03 (d, J = 3.7 Hz, 8H), 3.82 (d, J = 9.1 Hz, 8H), 3.61 (dd, J = 14.6, 8.1 Hz, 16H), 3.41 (dd, J = 18.1, 9.5 Hz, 16H), 3.27 (d, J = 9.2 Hz, 8H). ^{13}C NMR (125 MHz, $(CD_3)_2SO$): δ_C 101.94, 85.25, 72.38, 71.81, 71.08, 9.25.

γ-CD-(NH$_2$)$_8$. The initiator precursor **γ-CD-I$_8$** (0.50 g, 0.2297 mmol, 1 equiv.) was dissolved in ethylenediamine (13.78 g, 15.3 mL, 1000 equiv.). The reaction was stirred at 80 °C for 12 h. After completion of the reaction, the organic solvent and excess ethylenediamine were removed. The crude material was re-dissolved in a minimal amount of H_2O and precipitated by adding Me_2CO. The solid was collected and lyophilized to yield the product as a pale-yellow powder (0.30 g, 80% yield). ^{1}H NMR (500 MHz, D_2O): δ_H 5.36 – 5.01 (br, 8H), 4.19 – 3.79 (br, 16H), 3.63 – 3.41 (br, 16H), 3.04 – 3.69 (br, 32H). MALDI-TOF (m/z): found, 1655.9 $[M+Na]^+$; 1633.9 $[M+H]^+$; 1595.8 $[M+Na]^+$-60 (M_1, $NH_2CH_2CH_2NH_2$); 1573.8 $[M+H]^+$-M_1; 1535.7 $[M+Na]^+$-2M_1; 1513.8 $[M+H]^+$-2M_1; 1475.7 $[M+Na]^+$-3M_1; 1453.7 $[M+H]^+$-3M_1; 1393.6 $[M+H]^+$-4M_1. This data matches the previously reported data.[94]

γ-CD-Nb$_8$. To the mixture of **γ-CD-(NH$_2$)$_8$** (93.9 mg, 0.057 mmol, 1 equiv.) and **Nb-NHS** (150 mg, 0.471 mmol, 8.2 equiv.), DMF (anhydrous, 3 mL) and triethylamine (300 µL) were added. The reaction was stirred at 80 °C for 12 h. After completion of the reaction, the organic solvent was removed, the crude product was re-dissolved in a minimal amount of DMF and precipitated by adding Me_2CO. The precipitation was performed three times to yield the product as a brown solid (185 mg, 60% yield). ^{1}H NMR (500 MHz, $(CD_3)_2SO$): δ_H 8.19 – 7.79 (m, 8H), 6.30 (s, 16H), 5.22 – 4.75 (m, 8H), 4.67 – 4.14 (m, 8H), 4.13 – 3.46 (m, 32H), 3.43 – 1.96 (m, 112H), 1.82 – 1.57 (m, 8H), 1.40 – 1.25 (m, 8H).

General procedure for the synthesis of DBASCs

A solution of Grubbs 3rd generation catalyst[95] (G3G, 0.1 M) was freshly prepared in DMF. G3G (0.0245 mL, 1.78 mg, 2.45 µmol, 8 equiv.) was added to a solution of **γ-CD-Nb$_8$** (1.56 mM, 0.172 mL, 1.00 mg, 0.31 µmol, 1 equiv.) in DMF to give G3G: **γ-CD-Nb$_8$** ratio of 8:1. The resulting solution was stirred for 2 h at room temperature. The intermediate bearing eight initiated sites was confirmed by ^{1}H NMR using the styrene group from the initial ring-opening step with G3G. After that, **Nb-HEG** (10.49 mg, 24.54 µmol, 80 equiv.) was added and stirred at room temperature for 5 h, then **Nb-PEG** (54.42 mg, 24.54 µmol, 80 equiv.) was added and stirred for 3 h. The reaction was quenched by the addition of excess ethyl vinyl ether (EVE) and stirred for 30 min. Then, the excess EVE and DMF were removed by vacuum to yield the star polymer as a brown solid. For binding affinity, drug release and cytotoxicity studies, the polymer was first dialyzed against DMF (RC dialysis tubing, 1 kDa molecular weight cut-off, 38 mm flat-width) to remove the G3G catalyst residue, and then dialyzed against H_2O to remove DMF, the polymer inside the dialysis tubing was collected and lyophilized for 24 h.

Characterization of DBASC thermal properties and crystallinity

Thermogravimetric analysis (TGA) was performed on a TA Instruments TGA5000 using a high temperature platinum pan and 3 mg of sample that was heated from 25 to 800 °C at a rate of 10 °C/min. Differential scanning calorimetry (DSC) was performed on a TA Instruments DSC2500 with 18–22 mg of sample massed into a Tzero aluminum pan, which was sealed with a Tzero hermetic lid. Samples were first equilibrated at 200 °C for 10 minutes, followed by cooling to –50 °C at 5 °C/min, heating to 200 °C at 5 °C/min and cooling to –50 °C at 5 °C/min, data is reported from the second heating and cooling cycle. Powder X-ray diffraction (PXRD) was done using a Bruker d8 Advance X-ray diffractometer with zero background silicon sample holder (MTI), samples were prepared by grinding the as-synthesized polymers into a fine powder.

Procedure for HUVEC and MCF-7 cell culture

Human umbilical vein endothelial cells (HUVEC) and human breast cancer (MCF-7) cells were obtained from ATCC (American Type Culture Collection, USA) and were cultured as recommended. HUVEC cells were grown in vascular basal cell medium (ATCC) supplemented with 1% penicillin/streptomycin (100 units/mL and

0.1 mg/mL, respectively) and the endothelial cell growth kit-BBE (ATCC) which contains 0.2 % bovine brain extract, 5 ng/mL rh EGF, 10 mM L-glutamine, 0.75 units/mL heparin sulfate, 1 µg/mL hydrocortisone, 50 µg/mL ascorbic acid, and 2% fetal bovine serum. MCF-7 cells were grown in Dulbecco's Modified Eagle's Medium (DMEM) supplemented with 10% heat inactivated fetal bovine serum and 1% penicillin/streptomycin (100 units/mL and 0.1 mg/mL, respectively). All cells were maintained at 37 °C and 5% CO_2 in a humid incubator.

Procedure for determining DBASC cytotoxicity and efficacy

Cells (HUVEC and MCF-7) were seeded in a 96-well plate (5,000 cells/well, 100 µL) and incubated overnight to ensure proper attachment before treatment with various concentrations of empty **CD-(HEG$_7$-PEG$_9$)$_8$**, DOX·HCl loaded **CD-(HEG$_7$-PEG$_9$)$_8$**, and free DOX·HCl. Each polymer/drug combination and concentration were prepared and measured in four replicate wells. The final column contained four wells with cells (control) and four wells contained media only (blank). After 48 h of treatment, 100 µL of Celltiter Glo® (Promega) was added to each well and the luminescence was measured. Viability was calculated as follows:

$$\frac{Lum_{sample} - Lum_{blank}}{Lum_{control} - Lum_{blank}} \times 100 = \% \text{ Viability}$$

Results and discussion

Design and synthesis of well-defined γ-CD-based star polymers

The star polymer design and core-first/graft-from synthetic strategy described here is based on three main building blocks (Fig. 1a): *i)* a multifunctional initiator (**γ-CD-Nb$_8$**), *ii)* a norbornene-HEG monomer (**Nb-HEG**), and *iii)* a norbornene-PEG macromonomer (**Nb-PEG**). In the first step, **γ-CD-Nb$_8$** is activated by adding eight equiv. of Grubbs' 3rd generation catalyst in DMF at room temperature (Fig. 1b). Then, 8m·**Nb-HEG** is added to initiate polymerization of all eight arms, thus forming the homo-arm star polymer **CD-(HEG$_m$)$_8$**. Next, chain extension of the ω-functional arms is achieved by adding 8n·**Nb-PEG**, which produces the corresponding DBASC: **CD-(HEG$_m$-PEG$_n$)$_8$**.

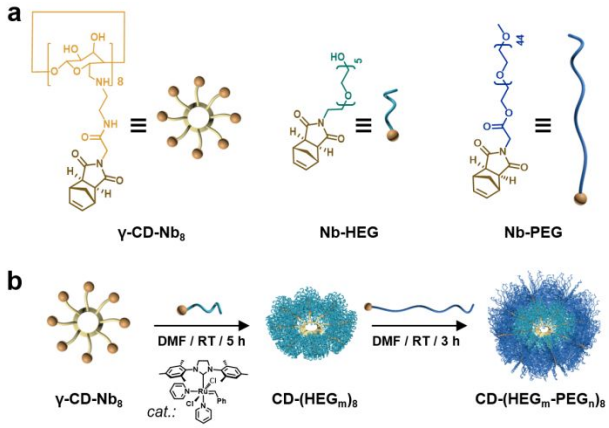

Fig. 1. (a) Chemical structures and corresponding cartoon representations of **γ-CD-Nb$_8$**, **Nb-HEG,** and **Nb-PEG**. (b) Core-first/graft-from synthetic strategy for DBASCs (**CD-(HEG$_m$-PEG$_n$)$_8$**).

To enable the synthesis of the water-soluble, eight-arm DBASCs, the primary alcohols of γ-CD were first converted to iodide leaving groups using triphenylphosphine (Scheme 1), followed by nucleophilic substitution using ethylene diamine in dimethylformamide (DMF). The desired product (**γ-CD-(NH$_2$)$_8$**) was obtained after each step by dissolving the crude mixture in minimal solvent and precipitating in excess acetone (Me_2CO) three times, where the overall yield for the first two steps was 47%. To install the norbornene groups onto **γ-CD-(NH$_2$)$_8$**, an *N*-hydroxysuccinimide precursor (**Nb-NHS**) was synthesized by coupling a norbornene-glycine (**Nb-Gly**) derivative (see Supporting Information (SI) for its preparation) to NHS using *N*,*N*′-dicyclohexylcarbodiimide (DCC) in dichloromethane (CH_2Cl_2) at room temperature (70% yield). Then, one equiv. of **γ-CD-(NH$_2$)$_8$** and a slight excess (8.2 equiv.) of **Nb-NHS** were reacted in the presence of triethylamine (TEA) in DMF at 80 °C. The desired product (**γ-CD-Nb$_8$**) was obtained by re-dissolving the concentrated crude material in a minimal amount of DMF, followed by precipitation in excess Me_2CO to obtain pure product as a brown solid (60% yield). See the SI (Schemes S1-4 and Fig. S3 and S10) for more details on the synthesis and characterization of the initiator.

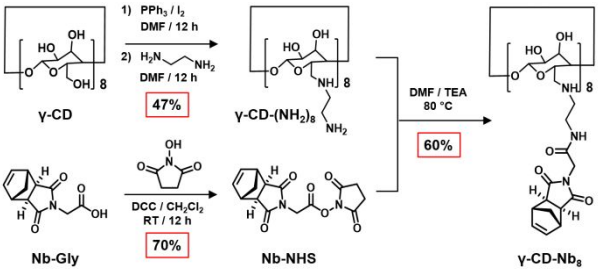

Scheme 1. Synthesis of multifunctional core initiator, **γ-CD-Nb$_8$**.

Next, the number of initiated sites on the core – and therefore the number of possible arms – was investigated by comparing the proton nuclear magnetic resonance (^{1}H NMR) spectra of the core precursors, **γ-CD-I$_8$** and **γ-CD-(NH$_2$)$_8$** (Fig. 2a-b), **γ-CD-Nb$_8$** (Fig. 2c), and the Grubbs' catalyst-initiated core, **i-γ-CD-Nb$_8$** (Fig. 2d). To generate the ring-opened initiator (Fig. 2, left), **γ-CD-Nb$_8$** was treated with eight equiv. of Grubbs' 3rd gen. catalyst for five hours, followed by quenching with ethyl vinyl ether (EVE), purification via dialysis against Me_2CO using low molecular weight cut-off tubing (MWCO = 1 kDa), and drying. The key proton resonances utilized in this analysis are the amide (7.75–8.50 ppm) and styrene (7.10–7.50 ppm) aromatic protons (blue and brown in Fig. 2d, respectively) associated with the linker and the ring-opening event. Although the amide peak broadens – due to hydrogen bonding and potential reversible encapsulation by CD – the relative integration is fairly accurate at approximately 8:40, which is the expected ratio if all sites on the core initiated properly. Further analysis of the ^{1}H NMR spectra reveals the resonance at ~6.3 ppm in Fig. 2c, which corresponds to the closed norbornene olefin protons, has fully converted to the *cis/trans* olefin stereoisomers (Fig. 2d). See also Fig. S1 for the full ^{1}H NMR spectra.

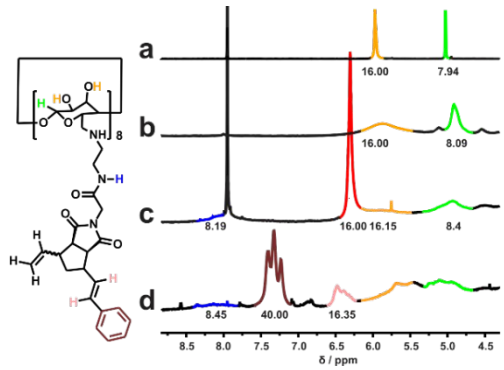

Fig. 2. ^{1}H NMR (500 MHz, 25 °C, $(CD_3)_2SO$) spectra of (a) **γ-CD-I$_8$**, (b) **γ-CD-(NH$_2$)$_8$**, (c) **γ-CD-Nb$_8$** and (d) the Grubbs' catalyst-initiated CD core **i-γ-CD-Nb$_8$**. The corresponding integral values are provided directly under each set of proton resonances.

bottom spectrum) appears to show complete consumption of the macromonomer, as evidenced by the disappearance of the characteristic norbornene olefin proton resonance at ~6.3 ppm. However, the corresponding GPC trace (Fig. 3c, black trace) shows some residual unreacted macromonomer is present. Even still, chain extension to obtain the desired DBASC is efficient (i.e., no visible **CD-(HEG$_7$)$_8$** peak observed by GPC). Also, as shown in Table 1, the number-average molecular weights calculated by NMR and GPC ($M_{n,NMR}$ = 187.3 kDa and $M_{n,GPC}$ = 177.8 kDa) are close to the theoretical number-average molecular weight ($M_{n,theo}$ = 214.8 kDa). Chain extensions with **Nb-PEG** to make the higher molecular weight DBASCs based on 20 and 30 equiv. of **Nb-HEG** were also carried out. Analysis of the corresponding GPC data (Fig. 3c and S4) shows successful incorporation of **Nb-PEG** into the arms of the narrowly dispersed star polymers, albeit not as efficient as in the case of the lower molecular weight DBASC. This statement is supported by the

Table 1. Molecular weight and dispersity determination of reported star polymers*

DBASCs (Theoretical)	DBASCs (Calculated$_{NMR}$)	Molecular Weight (kDa)				$DP_{n,NMR}$	$Đ_{,GPC}$
		$M_{n,theo}$	$M_{n,NMR}$	$M_{n,GPC}$	$M_{w,GPC}$		
CD-(HEG$_{10}$)$_8$	CD-(HEG$_5$)$_8$	37.46	20.36	27.09	30.33	40	1.120
CD-(HEG$_{20}$)$_8$	CD-(HEG$_7$)$_8$	71.66	28.48	44.69	50.67	59	1.134
CD-(HEG$_{30}$)$_8$	CD-(HEG$_{13}$)$_8$	105.9	47.71	47.44	54.18	104	1.142
CD-(HEG$_{50}$)$_8$	CD-(HEG$_{17}$)$_8$	174.3	60.54	56.97	66.24	134	1.163
CD-(HEG$_{70}$)$_8$	CD-(HEG$_{23}$)$_8$	242.7	82.77	79.65	93.75	186	1.177
CD-(HEG$_{10}$-PEG$_{10}$)$_8$	CD-(HEG$_7$-PEG$_9$)$_8$	214.8	187.3	177.8	198.5	57/72	1.117
CD-(HEG$_{20}$-PEG$_{20}$)$_8$	CD-(HEG$_5$-PEG$_{14}$)$_8$	426.4	262.0	329.9	377.3	40/109	1.144
CD-(HEG$_{30}$-PEG$_{30}$)$_8$	CD-(HEG$_9$-PEG$_{13}$)$_8$	637.9	267.7	396.7	473.3	74/105	1.193

*Note: The number of repeating units were rounded to the nearest number, which explains why the total DP$_n$ on the right – calculated from the non-rounded numbers – appears slightly higher/lower than the expected values that one would obtain using the subscripted numbers in the DBASC columns.

After confirming the number of initiation sites on the core, the efficiency of the first polymerization step was assessed by adding 10, 20, 30, 50, and 70 equiv. of **Nb-HEG** for each initiated site on **i-γ-CD-Nb$_8$** – i.e., 80, 160, 240, 300, and 560 total equiv. relative to the γ-CD core. The number of HEG subunits that were incorporated into the homo-arm star polymers (**CD-(HEG$_m$)$_8$**) was determined using

^{1}H NMR (Fig. 3a, Table 1, and Fig. S2 (full peak assignments)) and comparing the relative integration values for the diagnostic styrene proton resonances (Fig. 2d) and two methylene protons associated with the polymerized HEG (Fig. 3, resonance near 4.50 ppm). Although the results from the NMR analysis reveal incorporation of HEG subunits below the theoretical amount (Table 1, columns 1-2), the corresponding gel permeation chromatography (GPC) traces for each polymerization with **Nb-HEG** (Fig. 3b) illustrate narrow dispersities associated with the formation of each star polymer. Moreover, the molecular weight values obtained from NMR end-group analysis and SEC multiangle light-scattering (MALS) data from GPC are in good agreement.

Next, the living nature of the ω-functional arms was evaluated by adding 10, 20, and 30 equiv. of **Nb-PEG** macromonomer to each arm of the homo-arm star polymers that were set up initially with 10, 20, and 30 equiv. of **Nb-HEG** per initiation site. Analysis of a representative ^{1}H NMR spectrum for **CD-(HEG$_7$-PEG$_9$)$_8$** (Fig. 3a, fact that homo-arm star polymer precursors (**CD-(HEG$_m$)$_8$**) and unreacted **Nb-PEG** are both visible in the GPC traces shown in Fig. 3c (red and blue). Additionally, the molecular weight data in Table 1 shows calculated values for M_n (obtained from NMR and GPC) that are lower than $M_{n,theo}$. Along these lines, triblock brush-arm star polymers (TBASCs) were synthesized using a methyl-capped norbornene monomer in between HEG and PEG monomers. The corresponding GPC data (Fig. S5) shows similar conversion efficiencies that were observed for the higher molecular weight DBASCs. Thus, in the timeframe each polymerization was carried out, higher monomer/macromonomer conversion efficiencies are achievable at lower molecular weight diblock bottlebrush arms. It

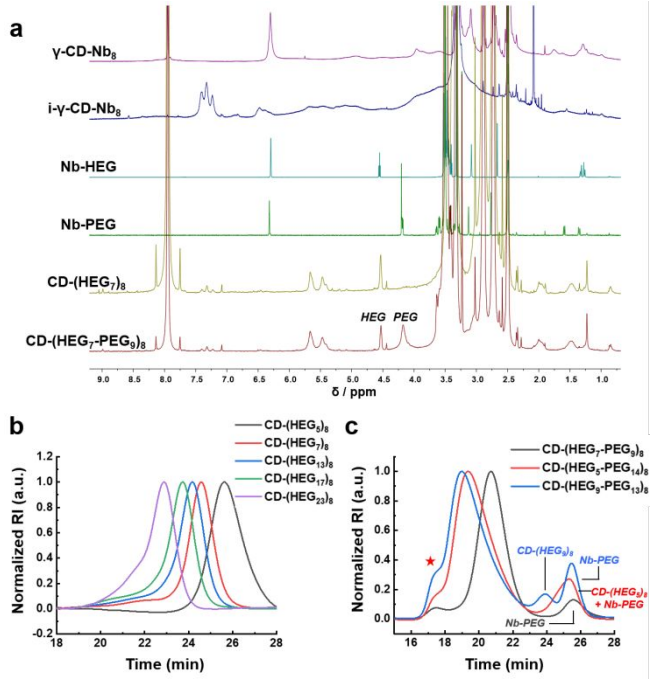

Fig. 3. (a) ^{1}H NMR spectra of core, initiated core, monomers, and star polymers (500 MHz, 25 °C, $(CD_3)_2SO$). (b) GPC traces of homo-arm star polymers (H_2O, 0.025 M Na_2SO_4, 50 °C). (c) GPC traces for all three DBASCs (same conditions). The red star in (c) presumably results from some aggregation of star polymers arising from analyte-column interactions. This was also observed for triblock-arm star polymers and star polymers generated with sub-stoichiometric amounts of Grubbs catalyst (Figs. S5 and S7, respectively).

is important to note that all molecular weight determinations by GPC used dn/dc values that were measured for **CD-(HEG$_5$)$_8$** and **CD-(HEG$_7$-PEG$_9$)$_8$** (Fig. S6).

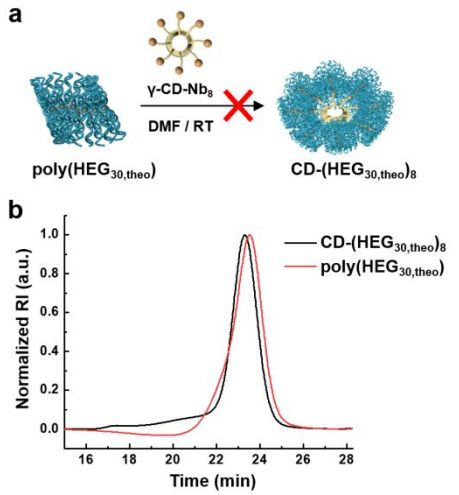

Fig. 4. (a) Illustration depicting an arm-first synthesis that was attempted to prepare DBASCs. (b) GPC data for the synthesized linear poly(HEG$_{30,theo}$) (red trace) and the resultant product after addition of the multifunctional core initiator **γ-CD-Nb$_8$** (black trace).

As a control experiment, an arm-first synthesis to prepare DBASCs was attempted (Fig. 4a), where poly(HEG$_{30,theo}$) was synthesized first, followed by crosslinking with the multifunctional core initiator **γ-CD-Nb$_8$** in the same ratio as the core-first approach (i.e., 8:1 arm:core). Analysis of the corresponding GPC data (Fig. 4b) reveals an unsuccessful crosslinking reaction, where only a slight shift to a higher molecular weight is observed. This small shift in molecular weight is likely due to the addition of only one or two poly(HEG$_{30,theo}$) onto **γ-CD-Nb$_8$**, indicating inefficient star polymer formation.

Similarly, another control experiment was performed, where a core-first/graft-from synthesis was initiated with a sub-stoichiometric amount of catalyst (two equiv. instead of eight), followed by the addition of 240 equiv. of **Nb-HEG**. The lack of complete initiation of each norbornene group on **γ-CD-Nb$_8$** resulted in apparent star-star coupling, as evidenced by the broad GPC peak at ~18.5 min (Fig. S7). For comparison, the core-first/graft-from synthesis with complete initiation of all norbornene groups yielded better control over the polymerization and resulted in more narrowly dispersed DBASCs with a retention time of ~24.0 min by GPC (Fig. 3b, blue trace).

Dimensions and physical properties of the well-defined DBASCs

Characterization of the dimensions and physical properties of the well-defined DBASCs was performed using dynamic light scattering (DLS), transmission electron microscopy (TEM), differential scanning calorimetry (DSC), thermal gravimetric analysis (TGA), and powder X-ray diffraction (PXRD). The morphology and size distribution of **CD-(HEG$_7$-PEG$_9$)$_8$** was first assessed by TEM (Fig. 5a). The deposition of the resultant star polymers on the TEM grid resulted in nanostructures that appeared crystalline and porous, adopting an almost "honeycomb" morphology. Analysis of the TEM data reveals a DBASC distribution (Fig. 5b) ranging from 5–30 nm in size, where the average size centred about 15 nm. In an aqueous solution, the three synthesized DBASCs possessed hydrodynamic diameters (D_h) between 10.0–11.0 nm at lower concentrations, where no aggregation was observed (Fig. 5c: **CD-(HEG$_7$-PEG$_9$)$_8$**; Fig. S8: all three DBASCs; Fig. S9: two TBASCs with D_h = 16.0–26.0 nm). Although these D_h values are smaller than that measured using TEM, it is expected that aggregation on the TEM grid will result in larger sizes.

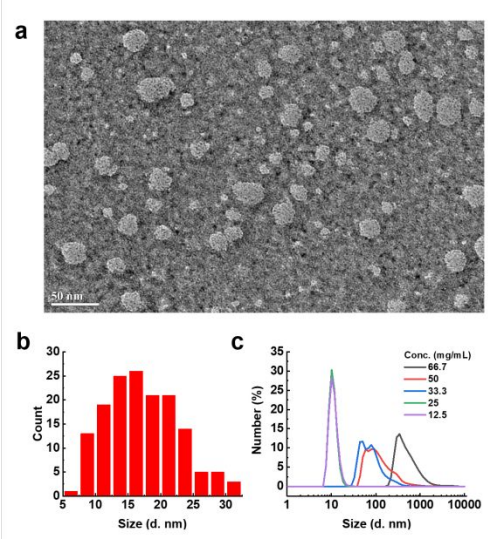

Fig. 5. (a) TEM image showing **CD-(HEG$_7$-PEG$_9$)$_8$** (lighter colored spherical shapes) on a 400 mesh Cu grid stained with an aqueous solution containing 2% uranyl acetate. (b) Size distribution of **CD-(HEG$_7$-PEG$_9$)$_8$** calculated from TEM image displays a range of singular star polymers and their corresponding aggregates. (c) Number (%) DLS plots of **CD-(HEG$_7$-PEG$_9$)$_8$** demonstrating

concentration-dependent aggregation in solution.

Next, the thermal properties of all three DBASCs (and two TBASCs) were assessed in the solid state. The temperature values for decomposition (T_d), glass transition (T_g), crystallization (T_c), and melting (T_m) were recorded from TGA (Fig. S11a) and DSC (Fig. 6a-b and S11b) and are listed in Table 2. In each category, the threshold temperatures declined as the arms of each star polymer became longer and higher in molecular weight. This trend implies that more disorder was introduced in between star polymers as additional HEG and PEG subunits were incorporated into the arms of each DBASC. A similar analysis of DSC data obtained (Fig. S12) for block copolymers that resembled the arms of each star polymer revealed a similar trend in decreasing thermal transition temperatures as the molar mass of the polymer increased, at least for the first two polymers that were synthesized. Interestingly, the block copolymer that was synthesized to resemble one arm of CD-$(HEG_9$-$PEG_{14})_8$ actually showed an increase in Tc and Tm, and which was more consistent with CD-$(HEG_7$-$PEG_9)_8$. Additionally, PXRD of each DBASC solid-state sample shows intense diffraction peaks at large scattering angles. Analysis of these results in conjunction with the DSC data further suggests that the DBASCs exhibit excellent packing in the solid-state and form well-ordered, highly crystalline domains. A more extensive investigation into the nano-based self-assembly of the reported DBASCs is currently underway in our laboratory.

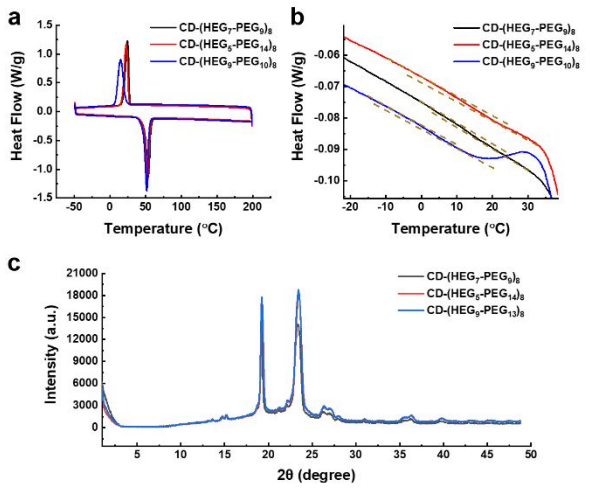

Fig. 6. (a) DSC data for all three DBASCs, exhibiting prominent peaks corresponding to T_c and T_m. (b) Zoom-in of DSC traces to illustrate how the T_g for each DBASC sample was determined. (c) PXRD data for each DBASC powder.

Table 2. Thermal transition temperatures of well-defined DBASCs.

DBASCs (Calculated$_{NMR}$)	Thermal Transition Temperature (°C)			
	T_g	T_c	T_m	T_d
CD-$(Heg_7$-$PEG_9)_8$	13	24.5	53.3	310
CD-$(Heg_5$-$PEG_{14})_8$	12	22.9	53.0	310
CD-$(Heg_9$-$PEG_{13})_8$	5	14.9	51.7	310

Binding affinity, cytotoxicity, and efficacy of DBASCs

Having established the synthesis, structure, and physical properties of each DBASC, their ability to function as a drug delivery vehicle was evaluated next. The larger γ-CD macrocycle was chosen over β-CD because its bigger cavity allows for stronger binding of hydrophobic drugs, such as DOX·HCl, which is sparingly soluble in DMSO:aqueous buffer solutions. To support this claim, a titration was carried out and monitored by ^{1}H NMR (Fig. S13-14), where DOX·HCl was titrated in aliquots of 0.1 equiv. into a 1 mM solution containing β-CD until two full equiv. were added. The same experiment was performed for γ-CD (Fig. S15-16), and the change in diagnostic proton resonances associated with each CD host was plotted to determine the corresponding affinity constants (K_a) (see Section F in the SI for a more thorough description). As expected, β-CD exhibited a binding affinity for DOX·HCl that was an order of magnitude lower than that obtained for the larger native γ-CD macrocycle (K_a = 10^2 versus 10^3 M^{-1}, respectively). Another set of titrations was also done with native γ-CD and **CD-$(HEG_7$-$PEG_9)_8$**, except instead of monitoring each by NMR, UV-Vis absorption spectroscopy was used instead (Fig. S17-19 and 7a-b). Similarly, the K_a values were calculated by plotting the change in absorbance at specific wavelengths as more guest (drug) was added to each host solution in concentrated aliquots. For both γ-CD and the DBASC, the binding affinity was found to be comparable (both 10^3 M^{-1}). However, we did observe two inflection points (at 1.0 and 2.5 equiv.) in the titration data (Fig. 7b) for the star polymer. We attribute this to the 1:1 binding by the γ-CD core, followed by residual binding by the star polymer's bulky diblock bottlebrush arms.

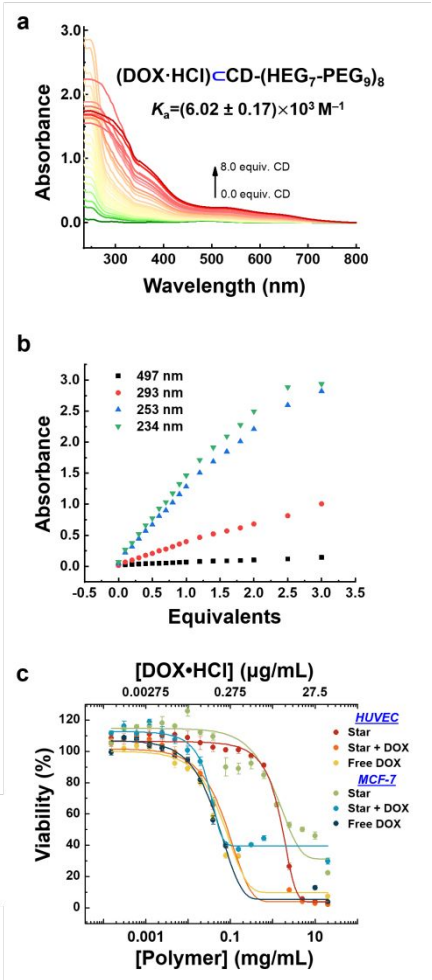

Fig. 7. (a) Host-guest binding affinity titration monitored by UV-Vis absorbance spectroscopy as an increasing number of equiv. of DOX·HCl was added to a 1 mM aqueous solution containing DBASC.

The binding affinity (K_a) was calculated by plotting the change in absorbance as a function of increasing concentrations of the guest (drug), where the data was entered and fitted using the resource supramolecular.org (see SI). (b) Change in absorbance (from Fig. 7a) plotted against number of equiv. of DOX·HCl added. (c) Cell viability plots for DBASC both empty and loaded with DOX·HCl, as well as with only free DOX·HCl, against a healthy HUVEC line and a breast cancer cell line (MCF-7).

To confirm the low toxicity of the DBASCs, a stock solution of **CD-(HEG$_7$-PEG$_9$)$_8$** (20 mg/mL) was diluted with media multiple times and incubated for 48 h with healthy human umbilical vein endothelial cells (HUVECs) in a 96-well plate (~5,000 cells/well). This experiment was also performed for the same DBASC loaded with DOX·HCl, as well as just for a solution containing free DOX·HCl. The results (Fig. 7b) of this viability assessment showed IC_{50} values of 1.64 mg/mL for empty DBASC and 0.08 mg/mL when loaded with one equiv. of the anticancer drug. The increased toxicity for the latter is expected considering DOX·HCl is an incredibly toxic drug. Comparing the DOX-loaded DBASC to free DOX·HCl, a higher concentration of the drug is needed to reach the IC_{50} value of HUVECs when bound by the DBASC versus the free drug (0.21 vs. 0.15 μg/mL of DOX). This lower toxicity is presumably due to the better solubility and slower release (Fig. S15) of the drug from the DBASC over time.

Lastly, the efficacy of the DBASC against MCF-7 was evaluated. Similar to the cytotoxicity studies, stock solutions of loaded and unloaded DBASC, as well as free DOX·HCl, were prepared and added to a 96-well plate containing the breast cancer cells (5,000 cells/well), followed by a 48 h incubation period. The live-dead cell viability assessment was carried out using a chemiluminescent assay and the results are plotted in Fig. 7c. Again, a higher concentration of the empty star polymer was needed to reach the IC_{50} value for MCF-7 cells in comparison to the DOX-loaded DBASC (0.87 vs. 0.03 mg/mL of star polymer). In terms of the DOX·HCl concentrations, only 0.09 μg/mL of drug bound by **CD-(HEG$_7$-PEG$_9$)$_8$** was needed to reach the IC_{50} value of MCF-7 cells, whereas 0.13 μg/mL of free DOX·HCl was needed to reach the same level. This greater potency may also likely be due to the enhanced solubility of the anticancer drug when bound by the star polymer under the experimental conditions described here. The difference in toxicity may also potentially be attributed to enhanced cellular uptake when bound by the polymer, but we did not confirm this hypothesis. Nonetheless, the results from these cytotoxicity and anticancer efficacy studies demonstrate how lower drug loadings are required for treatment when carried by the non-toxic DBASC drug delivery vehicle.

Conclusions

The synthesis, properties, and performance of a novel star polymer consisting of a γ-CD core and eight polynorbornene-based diblock brush-arm copolymers bearing HEG and PEG is described. Using ROMP, we demonstrated a core-first/graft-from approach to synthesize water-soluble DBASCs with high molar mass ($M_{n,NMR}$ = 187–268 kDa) and low dispersities ($Đ$ = 1.12–1.19). The D_h of the DBASCs were determined by DLS and found to be between 10.0–11.0 nm; a size which was corroborated by TEM measurements. The star polymer displayed well-ordered, crystalline domains in the solid state, as evidenced by prominent T_c and T_m peaks measured by DSC and intense diffraction peaks observed by PXRD. The enhanced ability of native γ-CD, as well as the γ-CD star polymer (**CD-(HEG$_7$-PEG$_9$)$_8$**) to bind the anticancer drug DOX·HCl was compared to native β-CD (10^3 vs. 10^2 M^{-1}, respectively), and the lower cytotoxicity of a representative DBASC (loaded and unloaded with DOX·HCl) was demonstrated against a healthy HUVEC line. The ability of the star polymers to bind and release DOX·HCl efficiently was also investigated against MCF-7 breast cancer cells and the drug-loaded star polymer showed greater potency than that of the free DOX·HCl treatment. We envision this γ-CD-based star polymer platform can function as a water-soluble and modular building block for potential applications in nanostructure self-assembly and drug delivery.

Conflicts of interest

The authors declare no conflicts.

Acknowledgements

We thank the Cancer Research Foundation for J.C.B.'s 2017 Young Investigator Award, which supported most of this research, and R. Alec and Anne Noel Dawson for their generous donation to the Barnes laboratory, which partially supported this research. We also thank Professor Richard Loomis for allowing us to use his lab's fluorimeter. A.O.D. also acknowledges support from the National Science Foundation Graduate Research Fellowship Program (NSF GRFP; DGE-1745038).

Notes and references

1. A. Blencowe, J. F. Tan, T. K. Goh and G. G. Qiao, *Polymer*, 2009, **50**, 5-32.
2. J. M. Ren, T. G. McKenzie, Q. Fu, E. H. H. Wong, J. Xu, Z. An, S. Shanmugam, T. P. Davis, C. Boyer and G. G. Qiao, *Chem. Rev.*, 2016, **116**, 6743-6836.
3. T. Masuda, Y. Ohta, T. Yamauchi and S. Onogi, *Polym. J. (Tokyo, Jpn.)*, 1984, **16**, 273-291.
4. H. Gao, *Macromol. Rapid Commun.*, 2012, **33**, 722-734.
5. Z. Li, E. Kesselman, Y. Talmon, M. A. Hillmyer and T. P. Lodge, *Science*, 2004, **306**, 98.
6. B. Chen, D. G. van der Poll, K. Jerger, W. C. Floyd, J. M. J. Fréchet and F. C. Szoka, *Bioconjugate Chem.*, 2011, **22**, 617-624.
7. W. Wu, W. Wang and J. Li, *Prog. Polym. Sci.*, 2015, **46**, 55-85.
8. T. Terashima, M. Kamigaito, K.-Y. Baek, T. Ando and M. Sawamoto, *J. Am. Chem. Soc.*, 2003, **125**, 5288-5289.
9. B. Helms, S. J. Guillaudeu, Y. Xie, M. McMurdo, C. J. Hawker and J. M. J. Fréchet, *Angew. Chem., Int. Ed.*, 2005, **44**, 6384-6387.
10. Y. K. Choi, Y. H. Bae and S. W. Kim, *Macromolecules*, 1998, **31**, 8766-8774.
11. W. R. Dichtel, K.-Y. Baek, J. M. J. Fréchet, I. B. Rietveld and S. A. Vinogradov, *J. Polym. Sci., Part A: Polym. Chem.*, 2006, **44**, 4939-4951.
12. S. Jang, H. C. Moon, J. Kwak, D. Bae, Y. Lee, J. K. Kim and W. B. Lee, *Macromolecules*, 2014, **47**, 5295-5302.
13. H. Gao and K. Matyjaszewski, *Macromolecules*, 2006, **39**, 7216-7223.
14. H. Gao and K. Matyjaszewski, *J. Am. Chem. Soc.*, 2007, **129**, 11828-11834.
15. J. Burdyńska, Y. Li, A. V. Aggarwal, S. Höger, S. S. Sheiko and K. Matyjaszewski, *J. Am. Chem. Soc.*, 2014, **136**, 12762-12770.
16. E. Altay and J. Rzayev, *Polymer*, 2016, **98**, 487-494.

17. S. Kanaoka, M. Sawamoto and T. Higashimura, *Macromolecules*, 1991, **24**, 2309-2313.
18. H. Shohi, M. Sawamoto and T. Higashimura, *Polym. Bull. (Berlin)*, 1991, **25**, 529-536.
19. R. Takahashi, M. Ouchi, K. Satoh, M. Kamigaito and M. Sawamoto, *Polym. J. (Tokyo, Jpn.)*, 1999, **31**, 995-1000.
20. N. Hadjichristidis, M. Pitsikalis, S. Pispas and H. Iatrou, *Chem. Rev.*, 2001, **101**, 3747-3792.
21. S. Aoshima and S. Kanaoka, *Chem. Rev.*, 2009, **109**, 5245-5287.
22. F. Wang, T. K. Bronich, A. V. Kabanov, R. D. Rauh and J. Roovers, *Bioconjugate Chem.*, 2005, **16**, 397-405.
23. D. J. A. Cameron and M. P. Shaver, *Chem. Soc. Rev.*, 2011, **40**, 1761-1776.
24. C. J. Hawker, *Angew. Chem., Int. Ed. Engl.*, 1995, **34**, 1456-1459.
25. A. W. Bosman, A. Heumann, G. Klaerner, D. Benoit, J. M. J. Fréchet and C. J. Hawker, *J. Am. Chem. Soc.*, 2001, **123**, 6461-6462.
26. K. Matyjaszewski, S. Qin, J. R. Boyce, D. Shirvanyants and S. S. Sheiko, *Macromolecules*, 2003, **36**, 1843-1849.
27. H. Gao and K. Matyjaszewski, *Prog. Polym. Sci.*, 2009, **34**, 317-350.
28. B. L. Buss, L. R. Beck and G. M. Miyake, *Polym. Chem.*, 2018, **9**, 1658-1665.
29. Y. Sudo, R. Kawai, Y. Nabae, T. Hayakawa and M.-a. Kakimoto, *Appl. Surf. Sci.*, 2019, **474**, 187-193.
30. H. W. Gibson, A. Farcas, J. W. Jones, Z. Ge, F. Huang, M. Vergne and D. M. Hercules, *J. Polym. Sci., Part A: Polym. Chem.*, 2009, **47**, 3518-3543.
31. F. Huang, D. S. Nagvekar, C. Slebodnick and H. W. Gibson, *J. Am. Chem. Soc.*, 2005, **127**, 484-485.
32. X. Huang, N. Zhang, L. Ban and H. Su, *Macromol. Rapid Commun.*, 2015, **36**, 311-318.
33. S. Angot, K. S. Murthy, D. Taton and Y. Gnanou, *Macromolecules*, 1998, **31**, 7218-7225.
34. C. Yang, H. Li, S. H. Goh and J. Li, *Biomaterials*, 2007, **28**, 3245-3254.
35. M. Zhang, Q. Xiong, J. Chen, Y. Wang and Q. Zhang, *Polym. Chem.*, 2013, **4**, 5086-5095.
36. M. E. Davis and M. E. Brewster, *Nat. Rev. Drug Discov.*, 2004, **3**, 1023-1035.
37. W. Saenger, J. Jacob, K. Gessler, T. Steiner, D. Hoffmann, H. Sanbe, K. Koizumi, S. M. Smith and T. Takaha, *Chem. Rev.*, 1998, **98**, 1787-1802.
38. K. Matyjaszewski and J. Xia, *Chem. Rev.*, 2001, **101**, 2921-2990.
39. K. Matyjaszewski, *Macromolecules*, 2012, **45**, 4015-4039.
40. K. Matyjaszewski and N. V. Tsarevsky, *Nat. Chem.*, 2009, **1**, 276.
41. T. G. Ribelli, F. Lorandi, M. Fantin and K. Matyjaszewski, *Macromol. Rapid Commun.*, 2019, **40**, 1800616.
42. P. Chmielarz, S. Park, A. Sobkowiak and K. Matyjaszewski, *Polymer*, 2016, **88**, 36-42.
43. K. Ohno, B. Wong and D. M. Haddleton, *J. Polym. Sci., Part A: Polym. Chem.*, 2001, **39**, 2206-2214.
44. F. J. Xu, Z. X. Zhang, Y. Ping, J. Li, E. T. Kang and K. G. Neoh, *Biomacromolecules*, 2009, **10**, 285-293.
45. B. J. Busche, A. E. Tonelli and C. M. Balik, *Polymer*, 2010, **51**, 454-462.
46. B. J. Busche, A. E. Tonelli and C. M. Balik, *Polymer*, 2010, **51**, 1465-1471.
47. B. J. Busche, A. E. Tonelli and C. M. Balik, *Polymer*, 2010, **51**, 6013-6020.
48. J. Li, Z. Guo, J. Xin, G. Zhao and H. Xiao, *Carbohydr. Polym.*, 2010, **79**, 277-283.
49. X. Pang, L. Zhao, M. Akinc, J. K. Kim and Z. Lin, *Macromolecules*, 2011, **44**, 3746-3752.
50. B. Huang, M. Chen, S. Zhou and L. Wu, *Polym. Chem.*, 2015, **6**, 3913-3917.
51. A. Wycisk, A. Döring, M. Schneider, M. Schönhoff and D. Kuckling, *Polymers*, 2015, **7**, 921-938.
52. N. Nafee, M. Hirosue, B. Loretz, G. Wenz and C. M. Lehr, *Colloids Surf., B*, 2015, **129**, 30-38.
53. Y. Wang, Y. Liu, J. Liang and M. Zou, *RSC Adv.*, 2017, **7**, 11691-11700.
54. F. Seidi, A. A. Shamsabadi, M. Amini, M. Shabanian and D. Crespy, *Polym. Chem.*, 2019, **10**, 3674-3711.
55. M. H. Stenzel and T. P. Davis, *J. Polym. Sci., Part A: Polym. Chem.*, 2002, **40**, 4498-4512.
56. L. Zhang and M. H. Stenzel, *Aust. J. Chem.*, 2009, **62**, 813-822.
57. P.-F. Gou, W.-P. Zhu, N. Xu and Z.-Q. Shen, *J. Polym. Sci., Part A: Polym. Chem.*, 2010, **48**, 2961-2974.
58. Q. Zhang, G.-Z. Li, C. R. Becer and D. M. Haddleton, *Chem. Commun. (Cambridge, U. K.)*, 2012, **48**, 8063-8065.
59. Y. Z. X. Lin, J. Ling, Z. Shen, *Macromol. Rapid Commun.*, 2012, **33**, 1008-1013.
60. Y. Miao, C. Rousseau, A. Mortreux, P. Martin and P. Zinck, *Polymer*, 2011, **52**, 5018-5026.
61. Z. Xu, S. Liu, H. Liu, C. Yang, Y. Kang and M. Wang, *Chem. Commun. (Cambridge, U. K.)*, 2015, **51**, 15768-15771.
62. K. Tungala, P. Adhikary, V. Azmeera, K. Kumar, K. Ramesh and S. Krishnamoorthi, *RSC Adv.*, 2016, **6**, 41594-41607.
63. F. Zhao, H. Yin, Z. Zhang and J. Li, *Biomacromolecules*, 2013, **14**, 476-484.
64. F. Zhao, H. Yin and J. Li, *Biomaterials*, 2014, **35**, 1050-1062.
65. R. H. Grubbs, *J. Macromol. Sci., Part A: Pure Appl. Chem.*, 1994, **31**, 1829-1933.
66. C. W. Bielawski and R. H. Grubbs, *Prog. Polym. Sci.*, 2007, **32**, 1-29.
67. M. M. Flook, L. C. H. Gerber, G. T. Debelouchina and R. R. Schrock, *Macromolecules*, 2010, **43**, 7515-7522.
68. M. M. Flook, V. W. L. Ng and R. R. Schrock, *J. Am. Chem. Soc.*, 2011, **133**, 1784-1786.
69. L. E. Rosebrugh, V. M. Marx, B. K. Keitz and R. H. Grubbs, *J. Am. Chem. Soc.*, 2013, **135**, 10032-10035.
70. Z. Li, K. Zhang, J. Ma, C. Cheng and K. L. Wooley, *J. Polym. Sci., Part A: Polym. Chem.*, 2009, **47**, 5557-5563.
71. Y. Xia, J. A. Kornfield and R. H. Grubbs, *Macromolecules*, 2009, **42**, 3761-3766.
72. M. J. Allen, K. Wangkanont, R. T. Raines and L. L. Kiessling, *Macromolecules*, 2009, **42**, 4023-4027.
73. A. J. Boydston, T. W. Holcombe, D. A. Unruh, J. M. J. Fréchet and R. H. Grubbs, *J. Am. Chem. Soc.*, 2009, **131**, 5388-5389.
74. J. A. Johnson, Y. Y. Lu, A. O. Burts, Y. Xia, A. C. Durrell, D. A. Tirrell and R. H. Grubbs, *Macromolecules*, 2010, **43**, 10326-10335.
75. V. Komanduri, D. R. Kumar, D. J. Tate, R. Marcial-Hernandez, B. J. Lidster and M. L. Turner, *Polym. Chem.*, 2019, **10**, 3497-3502.

76. G. C. Bazan and R. R. Schrock, *Macromolecules*, 1991, **24**, 817-823.
77. R. S. Saunders, R. E. Cohen, S. J. Wong and R. R. Schrock, *Macromolecules*, 1992, **25**, 2055-2057.
78. R. Learsch and G. M. Miyake, *J. Polym. Sci., Part A: Polym. Chem.*, 2018, **56**, 732-740.
79. J. Liu, A. O. Burts, Y. Li, A. V. Zhukhovitskiy, M. F. Ottaviani, N. J. Turro and J. A. Johnson, *J. Am. Chem. Soc.*, 2012, **134**, 16337-16344.
80. A. O. Burts, A. X. Gao and J. A. Johnson, *Macromol. Rapid Commun.*, 2014, **35**, 168-173.
81. L. Liao, J. Liu, E. C. Dreaden, S. W. Morton, K. E. Shopsowitz, P. T. Hammond and J. A. Johnson, *J. Am. Chem. Soc.*, 2014, **136**, 5896-5899.
82. J. C. Barnes, P. M. Bruno, H. V. T. Nguyen, L. Liao, J. Liu, M. T. Hemann and J. A. Johnson, *J. Am. Chem. Soc.*, 2016, **138**, 12494-12501.
83. Y. Shibuya, H. V. T. Nguyen and J. A. Johnson, *ACS Macro Letters*, 2017, **6**, 963-968.
84. H. V. T. Nguyen, Q. Chen, J. T. Paletta, P. Harvey, Y. Jiang, H. Zhang, M. D. Boska, M. F. Ottaviani, A. Jasanoff, A. Rajca and J. A. Johnson, *ACS Cent. Sci.*, 2017, **3**, 800-811.
85. M. R. Golder, H. V. T. Nguyen, N. J. Oldenhuis, J. Grundler, E. J. Park and J. A. Johnson, *Macromolecules*, 2018, **51**, 9861-9870.
86. H. V. T. Nguyen, A. Detappe, N. M. Gallagher, H. Zhang, P. Harvey, C. Yan, C. Mathieu, M. R. Golder, Y. Jiang, M. F. Ottaviani, A. Jasanoff, A. Rajca, I. Ghobrial, P. P. Ghoroghchian and J. A. Johnson, *ACS Nano*, 2018, **12**, 11343-11354.
87. M. R. Golder, J. Liu, J. N. Andersen, M. V. Shipitsin, F. Vohidov, H. V. T. Nguyen, D. C. Ehrlich, S. J. Huh, B. Vangamudi, K. D. Economides, A. M. Neenan, J. C. Ackley, J. Baddour, S. Paramasivan, S. W. Brady, E. J. Held, L. A. Reiter, J. K. Saucier-Sawyer, P. W. Kopesky, D. E. Chickering, P. Blume-Jensen and J. A. Johnson, *Nat. Biomed. Eng.*, 2018, **2**, 822-830.
88. K. Nomura, Y. Watanabe, S. Fujita, M. Fujiki and H. Otani, *Macromolecules*, 2009, **42**, 899-901.
89. K. Nomura, K. Tanaka and S. Fujita, *Organometallics*, 2012, **31**, 5074-5080.
90. K. Takamizu and K. Nomura, *J. Am. Chem. Soc.*, 2012, **134**, 7892-7895.
91. Z. Sun, K. Morishita and K. Nomura, *Catalysts*, 2018, **8**, 670.
92. Z. Sun and K. Nomura, *RSC Adv.*, 2018, **8**, 27703-27708.
93. S. Xiao, L. Si, Z. Tian, P. Jiao, Z. Fan, K. Meng, X. Zhou, H. Wang, R. Xu, X. Han, G. Fu, Y. Zhang, L. Zhang and D. Zhou, *Biomaterials*, 2016, **78**, 74-85.
94. N. Mourtzis, M. Paravatou, I. M. Mavridis, M. L. Roberts and K. Yannakopoulou, *Chem. Eur. J.*, 2008, **14**, 4188-4200.
95. J. A. Love, J. P. Morgan, T. M. Trnka and R. H. Grubbs, *Angew. Chem., Int. Ed.*, 2002, **41**, 4035-4037.

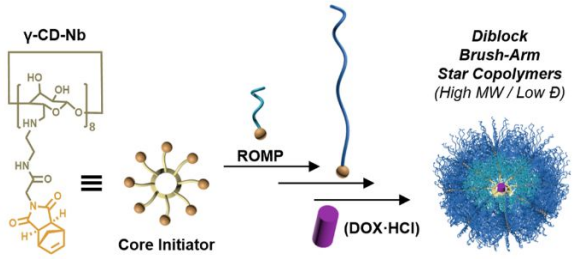

Water-soluble diblock arm star copolymers using *γ*-CD-based core-first ring-opening metathesis polymerization, allowing for anticancer drug delivery via host-guest interaction.